Chinese Chemical Letters 35 (2024) 108545

Contents lists available at ScienceDirect

Chinese Chemical Letters

journal homepage: www.elsevier.com/locate/cclet

H_2S-releasing adhesive hydrogel as oral radioprotectant for gastrointestinal tract radioprotection

Peng Shan[a,b,1], Jing Liao[a,b,1], Jiayi Li[a,1], Chengyan Wang[b,c], Jie Zhou[b], Linqiang Mei[b], Yunlu Dai[d], Qiang Wang[a,*], Wenyan Yin[b,*]

[a] *Laboratory for Micro-sized Functional Materials, Department of Chemistry and College of Elementary Education, Capital Normal University, Beijing 100048, China*

[b] *CAS Key Laboratory for Biomedical Effects of Nanomaterials and Nanosafety, Institute of High Energy Physics, Chinese Academy of Sciences, Beijing 100049, China*

[c] *Department of Pharmacy, Southwest Hospital, The Third Military Medical University, Chongqing 400038, China*

[d] *Cancer Centre and Institute of Translational Medicine, Faculty of Health Sciences, University of Macau, Macau SAR 999078, China*

ARTICLE INFO

Article history:
Received 13 February 2023
Revised 4 May 2023
Accepted 7 May 2023
Available online 9 May 2023

Keywords:
Radiation
Gastrointestinal tract radioprotection
Hydrogen sulfide gas therapy
Gelatin-based hydrogel
Free radicals scavenging

ABSTRACT

Radiation damage can cause a series of gastrointestinal (GI) tract diseases. The development of safe and effective GI tract radioprotectants still remains a great challenge clinically. Here, we firstly report an oral radioprotectant Gel@GYY that integrates a porous gelatin-based (Gel) hydrogel and a pH-responsive hydrogen sulfide (H_2S) donor GYY4137 (morpholin-4-ium 4 methoxyphenyl(morpholino) phosphinodithioate). Gel@GYY has a remarkable adhesion ability and long retention time, which not only enables responsive release of low-dose H_2S in stomach and subsequently sustained release of H_2S in the whole intestinal tract especially in the colon, but also ensures a close contact between H_2S and GI tract. The released H_2S can effectively scavenge free radicals induced by X-ray radiation, reduce lipid peroxidation level, repair DNA damage and recover vital superoxide dismutase and glutathione peroxidase activities. Meanwhile, the released H_2S inhibits radiation-induced activation of nuclear factor κB (NF-κB), thus reducing inflammatory cytokines levels in GI tract. After treatment, Gel@GYY displays efficient excretion from mice body due to its biodegradability. This work provides a new insight for therapeutic application of intelligent H_2S-releasing oral delivery system and potential alternative to clinical GI physical damage protectant.

Radiotherapy is one of the most frequently-used strategies in the clinical treatment of malignant tumors [1,2]. During radiotherapy of abdominal tumors, intestine is one of the main sensitive tissues to radiation [3]. In particular, due to the migration of tumor sites, constant changes in radiotherapy area will inevitably cause damage to the surrounding normal gastrointestinal (GI) tract tissues. Consequently, many radiation side effects including GI hemorrhage, gastroenteritis, nausea, and vomiting, reduce the quality of life of patients [4]. At present, radioprotectants are mainly divided into sulfur compounds (amifostine) [5,6], polyphenols (curcumin, tea polyphenol) [7], vitamins [8], trace element-based compounds [9], hormone analogues [10], and glutathione (GSH) [11]. Short half-life amifostine is currently used to protect against clinical head and neck tumor patients *via* intravenous injection. However, it cannot be available for oral administration clinically. In a Phase II clinical trial, a combination of pentoxifylline and vitamin E showed protective efficacy against superficial radiation-induced fibrosis [12]. A superoxide dismutase (SOD) mimics, BMX-001, has been verified as a potent radioprotectant in clinical trials [13]. Moreover, carbon-based nanomaterials [14], cerium-based nanomaterials [15,16], transition-metal dichalcogenides [17–19], and noble metal nanomaterials [20] have also great potential as radioprotectants. However, most preclinical and clinical radioprotectants are required short intervals of frequent intravenous administration with large side effects even very short retention time for GI tract protection. Oral administration is the most convenient approach with well patient-based compliance because of its advantages in improving bioavailability and distribution, noninvasiveness and fast reaching GI tract of therapeutic drugs [21]. Therefore, it is of great importance to explore safely and orally administrated radioprotectants for comprehensive GI tract protection.

* Corresponding authors.
E-mail addresses: qwchem@gmail.com (Q. Wang), yinwy@ihep.ac.cn (W. Yin).

[1] These authors contributed equally to this work.

https://doi.org/10.1016/j.cclet.2023.108545
1001-8417/

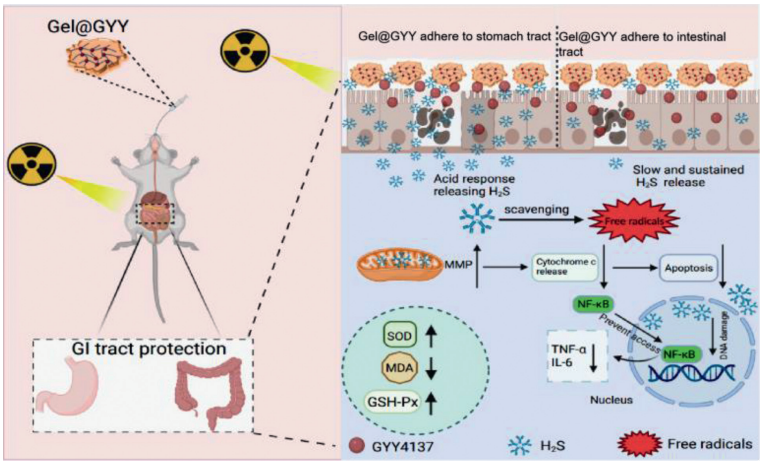

Scheme 1. Schematic diagram of the protection of GI tract damaged by X-ray. Adhesive Gel@GYY hydrogel as an oral radioprotection agent can responsively release H_2S in the gastric acid environment and sustained release H_2S in the whole intestinal tract, especially in the colon to effectively scavenge free radicals, retain in the GI tract for sufficient time, suppress inflammatory factors, recover SOD and GSH-Px activity, decrease lipid peroxidation, consequently alleviating the radioactive gastroenteritis.

Hydrogen sulfide (H_2S) is the third endogenous gas signal molecule after NO and CO, and it has numerous profound actions in mammalian physiology [22]. Endogenous H_2S is primarily produced from cysteine or cysteine derivatives in the mitochondria or cytosol [23]. H_2S delivery systems have potential for clinical applications to cure many diseases [24]. The key roles of H_2S include inhibiting oxidative stress, regulating mitochondrial function and reducing lipid peroxidation (LPO) levels [25]. H_2S also has the ability of treating cardiovascular disease [26], protecting organ ischemia and reperfusion from injury [27], treating central nervous system diseases [28], bio-imaging [29], anti-cancer [30,31] and anti-inflammatory [32,33]. At present, H_2S has made some clinical progress in the treatment of cardiovascular diseases and hypertension [34]. H_2S donors that are the compounds with the ability of releasing H_2S become very useful for various treatments. Roughly, they are divided into sulfide salts (Na_2S_x), morpholin-4-ium-4-methoxyphenyl (morpholino) phosphinodithioate (GYY4137, for short GYY), carlic-derived sulfur compounds, H_2S-hybrid nonsteroidal anti-inflammatory drugs (NSAIDs, photolabile H_2S donors, *etc*. As a typical H_2S donor, SG1002 (Phase I clinical trial of a H_2S prodrug) can produce H_2S in plasma and has made preliminary clinical progress for treatment of congestive heart failure [35]. In particular, ATB-346, a derivative of NSAIDs that composes of H_2S donor has also entered Phase II clinical practice [36]. However, for majority of H_2S donors, the drawbacks of quick and uncontrollable delivery and release of H_2S, short lifespan of H_2S limited their further bioapplications. Directional delivery of H_2S donors and controlled release of H_2S remain formidable challenges. GYY is a water-soluble, sustained-release H_2S donor. The release of H_2S from GYY has a unique characteristic of slow release of pH-response and temperature-dependence, especially at physiological 37 °C, which displays great potential to better simulate the time course of naturally produced H_2S release in the in intestinal tract [37]. When administrated into animals, GYY can cause and maintain elevated H_2S levels for a long period of time. Necessarily, selecting an appropriate delivery system for loading GYY with responding to the GI tract biological barrier becomes a major concern. Given this, we anticipate that the main goal is constructing an oral H_2S delivery system based on GYY to solve the specific issue of whole GI tract protection after radiotherapy.

In this work, we firstly constructed an oral GI radioprotectant (Gel@GYY) comprising porous gelatin-based (Gel) hydrogel loaded H_2S donor GYY (Scheme 1). As a clinically approved pharmaceutic adjuvant [38–41], the Gel offers several indispensable merits to the GYY. In our design, porous structure of the Gel can act as a carrier with low toxicity and biodegradability *in vivo*. Moreover, the Gel has good adhesion ability, long retention time and hemostatic function to the GI tract. Importantly, Gel@GYY can responsively release exogenous H_2S in acidic stomach and sustained release H_2S in the whole intestine. The good adhesion ability and gradual degradation ensure close contact and retention of H_2S in the local GI tract and adequate utilization of H_2S, consequently improving bioavailability of Gel@GYY. The released H_2S from Gel@GYY can effectively scavenge free radicals produced by radiation, reduce oxidative stress and DNA damage, and recover vital SOD and glutathione peroxidase (GSH-Px) homeostasis. Moreover, the sustained release of H_2S triggers the inhibition of activation of a pleiotropic nuclear factor κB (NF-κB) and transcriptionally exerts important antiinflammatory actions by suppressing downstream pro-inflammatory cytokines like interleukin-6 (IL-6) and tumor necrosis factor (TNF-α), alleviating the radioactive gastroenteritis. Consequently, the Gel@GYY presents an effective radioprotection to the whole GI tract especially to colon, prolonging the survival rate of mice after being exposed to a high X-ray dose (17 Gy). This work not only provides a safe yet effective pH-responsive and sustained H_2S-releasing radioprotectant but also shows potential alternative for clinical transformation of oral GI tract physical damage protectant.

The whole synthesis flowchart of Gel@GYY was shown in Fig. S1 (Supporting information). First, gelatin nanoparticles (NPs) were synthesized by a modified nanoprecipitation crosslinking method under acidic condition [42]. Then, the Gel hydrogel with an ointment-like appearance was formed when the pH was adjusted to 7 (Fig. S2a in Supporting information). The pH-sensitive behavior of the Gel hydrogel could endow it with more opportunities for controllable drug delivery. Moreover, the drug release rate of Gel hydrogel in the acidic medium is small, which can be used to prevent the rapid release of drugs in the harsh acidic environment of the stomach [43]. Transmission electron microscopy (TEM) image in Fig. 1a showed that the Gel NPs were spherical with good dispersion and the average particle size was 30 nm. Field emission scanning electron microscopy (FE-SEM) image in Fig. 1b presented a porous network structure with a size of several hundred microns, indicating the successful synthesis of Gel hydrogel after adjusting pH to 7. We then tested the zeta potentials before and after Gel hydrogel loading GYY. In Fig. 1c, the zeta potentials of Gel hydrogel and GYY were +20 mV and −23 mV, respectively. After loading GYY to Gel hydrogel, the zeta potential of Gel@GYY changed to −8 mV,

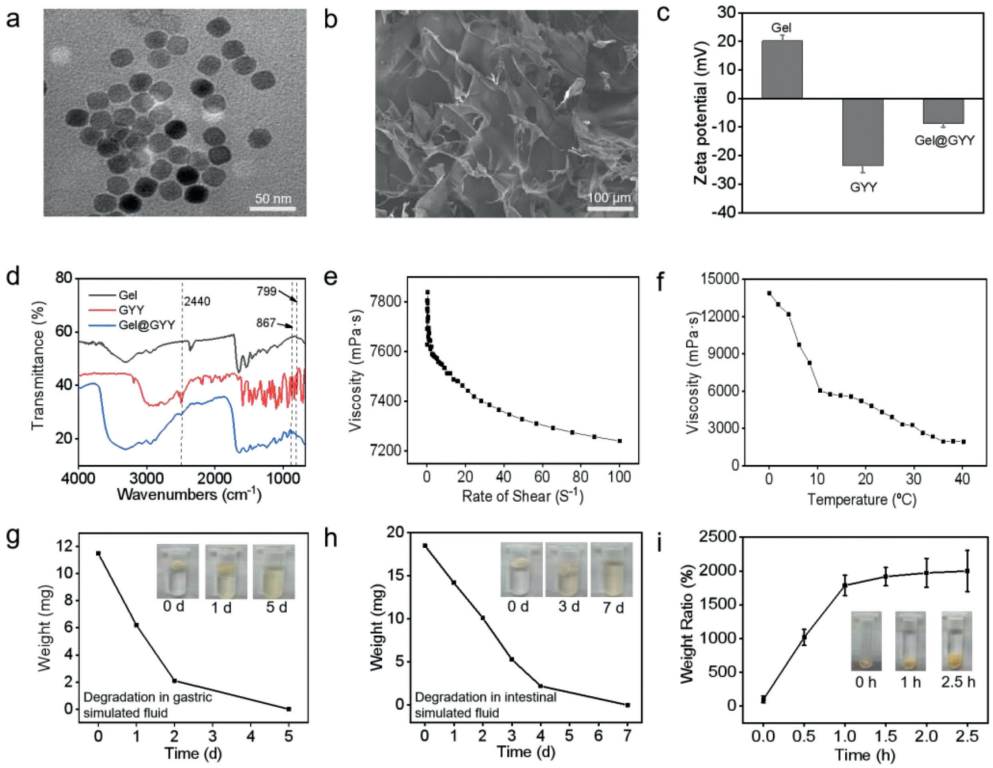

Fig. 1. Characterizations of Gel and Gel@GYY. (a) TEM image of Gel NPs. (b) FE-SEM image of porous Gel. (c) Zeta potential of Gel, GYY and Gel@GYY. (d) Micro-FTIR spectra of Gel, GYY and Gel@GYY. (e) Viscosity change at various shear rates. (f) Viscosity change at various temperatures. (g) Degradation of freeze-dried Gel in gastric simulants. Inset: Photographs of the degradation process, illustrating that the Gel can gradually degrade in a gastric acid environment for 5 at least days. (h) Degradation of lyophilized Gel in an intestinal fluid simulant. Inset: Photographs of lyophilized Gel ointment degradation process, illustrating that the Gel can gradually degrade in intestinal simulant within 7 days. (i) Swelling property of the Gel. Inset: Direct observation of the swelling characteristic of the lyophilized Gel in PBS buffer. Data represent mean ± standard error of the mean ($n = 3$).

further proving the successful loading of GYY with Gel hydrogel. Therefore, the negatively charged GYY (Fig. S2b in Supporting information) loaded on the positively charged Gel hydrogel to obtain Gel@GYY (Fig. S2c in Supporting information) could be due to electrostatic interaction and physical absorption. FE-SEM image in Fig. S3 (Supporting information) showed that the Gel@GYY remained a similar porous mesh structure to the Gel hydrogel in Fig. 1b. The negatively charged characteristic would be favorable for Gel@GYY adhering to the positively charged inflammatory site of colon *via* electrostatic interaction [44]. Moreover, the loading dose of GYY in the Gel hydrogel can be controlled by regulating the ratio of GYY and Gel hydrogel.

Next, micro Fourier transform infrared (Micro-FTIR) spectrum (Fig. 1d) of Gel hydrogel demonstrated a broadband of 3600–3300 cm^{-1}, which was attributed to -NH_2 group [45]. Compared to Gel hydrogel, the Micro-FTIR spectrum of Gel@GYY in Fig. 1d showed three additional peaks at 867, 799 and 2440 cm^{-1}, which were attributed to the para-substituted aromatic ring, -NH_2 and -P on GYY, respectively. This result further indicated that GYY was successfully loaded on the Gel hydrogel. We then tested the rheological properties of Gel hydrogel. Fig. 1e showed that the viscosity of Gel hydrogel decreased with the increase of rate of shear at 37 °C, indicating its state as a pseudoplastic fluid with good adhesion ability [46]. In Figs. S4a and b (Supporting information), we directly verified the viscosity of the Gel NPs and Gel hydrogel by comparing their fluidity before and after gelation. The adhesive properties of Gel hydrogel were also observed from the adhesion photos of gloves, skin (Fig. S4b) and biological tissues (Fig. S5 in Supporting information). This good adhesion of the Gel hydrogel is beneficial for its subsequent application in the GI tract. As shown in Fig. 1f, viscosity of the Gel hydrogel decreased with increasing temperature in the range of 0 °C to 40 °C, indicating that temperature affected its viscosity properties. Fig. S4c (Supporting information) showed that the Gel hydrogel changed from a paste-like state to a slowly viscous flow state (pseudoplastic fluid) within 48 h at 37 °C in a gastric acid simulated environment (pH 2) and an intestinal tract simulated environment (pH 8.4). To illustrate its biodegradation ability, we freeze-dried the Gel hydrogel and placed it in the simulated fluids of stomach and intestinal tract. Fig. 1g showed that the freeze-dried Gel hydrogel was gradually degraded in the gastric simulant at 37 °C on day 5. In the intestinal simulant, the freeze-dried Gel hydrogel was gradually degraded at 37 °C on day 7 (Fig. 1h). The gradual biodegradation properties of Gel hydrogel provide strong evidence for its biosafety. Next, we tested the water content of Gel hydrogel. At 70 °C, the wet Gel hydrogel (m_{wet}) gradually evaporated and dried to become a dry Gel hydrogel (m_{dry}) within 24 h As shown in Fig. S6 (Supporting information), the water content of Gel hydrogel declined with prolonged time which was calculated to be 96%. Fig. 1i showed the dried Gel hydrogel retains the capacity in absorbing water and swell in phosphate buffer saline (PBS) at 50 °C. Consequently, the mass did not change at 2.5 h, indicating that water absorption saturation reached the maximum degree owing to swelling effect. The temperature at 50 °C can cause the increase of diffusion rate of PBS to the hydrogel. Consequently, the swelling rate was as high as 2000%. The good adhesion in the GI tract, easy swelling and biodegradability lay a foundation for subsequent *in vivo* oral application.

Free radical scavenging is an effective approach to radiation protection [47]. GSH has a strong free radical scavenging ability that is widely used as antioxidant [48]. Therefore, the potential free radical scavenging ability of Gel@GYY was evaluated and compared with GSH. First, we choose two free radical models,

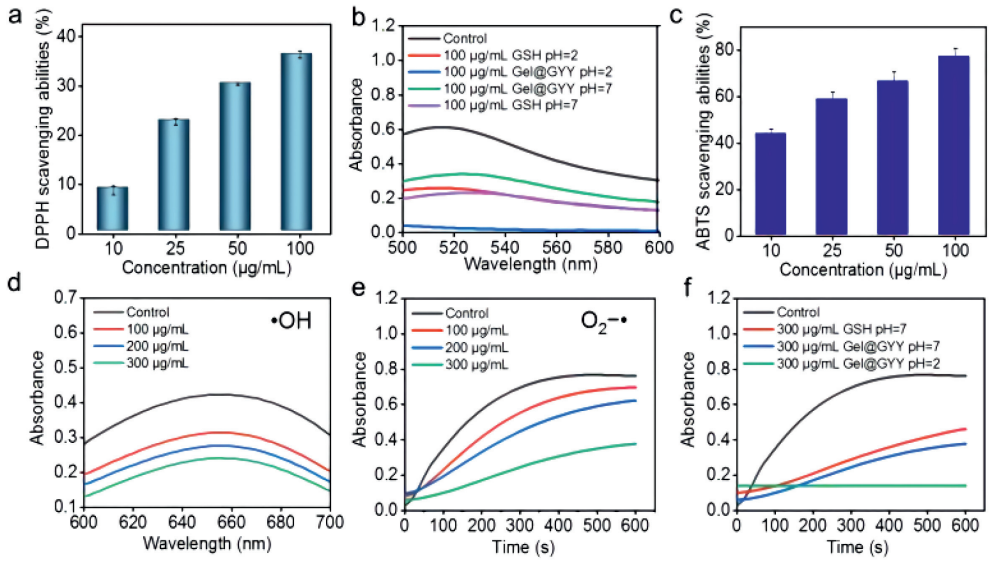

Fig. 2. Free radicals scavenging ability *in vitro*. (a) DPPH scavenging ability of Gel@GYY at pH 7. (b) Comparison of DPPH scavenging ability of Gel@GYY with GSH at pH 2 or pH 7. (c) ABTS scavenging ability of Gel@GYY at pH 7. (d) $^{\bullet}OH$ scavenging ability of Gel@GYY at pH 7. (e) $O_2^{-\bullet}$ scavenging ability of Gel@GYY at pH 7. (f) Comparison of $O_2^{-\bullet}$ scavenging ability of Gel@GYY with GSH at pH 2 or pH 7. Gel@GYY concentrations refer to the concentration of loaded GYY. Data represent mean ± standard error of the mean ($n = 3$).

1,1-diphenyl-2-picrylhydrazyl (DPPH) radical and 2,2′-azinobis(3-ethylbenzthiazoline-6-sulfonate) (ABTS) radical. The DPPH and ABTS radical scavenging effects obviously enhanced with the increased concentration of Gel@GYY (Figs. 2a and c). In Fig. 2b and Fig. S7 (Supporting information), the DPPH scavenging ability of Gel@GYY was not as high as that of GSH at pH 7. However, under acidic pH 2, the sudden decrease of absorbance for the Gel@GYY group indicated that the Gel@GYY has a higher DPPH scavenging ability than that of GSH. The comparison of DPPH scavenging ability of GSH with Gel@GYY at different pH treatments also indicated Gel@GYY has a higher DPPH radical scavenging efficiency in simulated gastric acid (pH 2) than that of GSH. This result further revealed that Gel@GYY has the ability of pH-responsive release of H_2S to scavenge free radicals.

Then, we further evaluated the scavenging ability of Gel@GYY to hydroxyl radicals ($^{\bullet}OH$) and superoxide radicals ($O_2^{-\bullet}$), which are the main free radicals produced in radiotherapy [13]. The absorbance of blue oxidized TMB (oxTMB) was generated by the reaction of $^{\bullet}OH$ with 3,3′,5,5′-tetramethylbenzidine (TMB) in the control group. After the addition of Gel@GYY, the lower absorbance reflected the stronger $^{\bullet}OH$ scavenging ability (Fig. 2d). Furthermore, in the control group, the absorbance at 560 nm appeared due to the reaction of $O_2^{-\bullet}$ with nitroblue tetrazoliumchloride (NBT). In contrast, the absorbance at 560 nm obviously decreased after the addition of Gel@GYY, suggesting that the $O_2^{-\bullet}$ scavenging ability of Gel@GYY became stronger than that of the control group (Fig. 2e). Also, with the increased concentration of Gel@GYY, the $^{\bullet}OH$ and $O_2^{-\bullet}$ scavenging ability also increased. Especially, in simulated gastric acidic pH 2, Gel@GYY still has obviously stronger $O_2^{-\bullet}$ scavenging ability than that of the GSH in pH 7 at the same concentration (Fig. 2f). The above results indicated that Gel@GYY has great potential for radioprotection of GI tract due to their pH- and concentration-dependent free radicals scavenging activities.

As previously mentioned, GYY is a pH-responsive and slow-releasing H_2S donor. Therefore, we next determined H_2S release from GYY using a 5,5′-dithiobis(2-nitrobenzoic acid) (DTNB) assay under acidic (pH 2) and weak alkaline (pH 8.4) PBS buffers, which are corresponding to the simulate stomach and an intestinal tract fluids, respectively. The product of the reaction of H_2S and DTNB has a typical absorption peak at 412 nm. In Fig. S8a (Supporting information), the absorption was measured under pH 2 after different reaction times between Gel@GYY and DTNB. Then, the amount of H_2S released from Gel@GYY can be calculated from the standard curve (Figs. S9a and b in Supporting information). It was calculated that 176 μmol/L of Gel@GYY continuously released 32 μmol/L of H_2S at pH 2 with prolonged time (Fig. S8b in Supporting information). Next, we tested the release of H_2S from Gel@GYY at pH 8.4 (Fig. S8c in Supporting information). In Fig. S8d (Supporting information), Gel@GYY cumulatively released about 4 μmol/L of H_2S from 176 μmol/L of Gel@GYY at pH 8.4 with prolonged time. The result indicated that the released H_2S at pH 2 was approximately 8-fold higher than at pH 8.4. Therefore, acidic condition accelerated the release of H_2S from the Gel@GYY and the Gel@GYY had the ability of releasing H_2S continuously at pH 8.4. The pH-responsive and sustained released dose of H_2S from Gel@GYY not only responded to the GI tract, but also ensured the radiation protection of the whole GI tract.

Radioprotection of Gel@GYY to intestinal crypt epithelial (IEC-6) cells was performed by live-dead staining (Fig. 3a). The green and red represent live cells and dead cells, respectively. It was found that the proportion of live cells in X-ray + Gel@GYY group was obviously higher than that of the X-ray group. But the percentage of live cells in the X-ray + Gel group had no distinct difference from the X-ray group. The results indicated that Gel@GYY can well reduce the cell death caused by X-ray irradiation. Then, clonal survival assays were performed to assess the colony-forming ability of IEC-6 cells cultured with Gel@GYY. As shown in Figs. 3b and c, when exposed to X-ray at 6 Gy, the cell survival was significantly decreased to 25% in the X-ray group compared to the control group. In contrast, cell survival rate of the X-ray + Gel@GYY group increased to 52%, implying that Gel@GYY can ultimately relieve X-ray-induced radiation damage. Subsequently, cell counting kit-8 (CCK-8) assay was used to perform the cell survival rate with/without Gel@GYY treatment at different times under X-ray irradiation. In Fig. 3d, the survival rate of IEC-6 cells in the X-ray + Gel@GYY group was significantly higher than that of the X-ray group, indicating that the Gel@GYY can sharply reduce damage caused by radiation and improve protective effect of radiotherapy.

Washington State Probe-5 (WSP-5) was used to detect the fluorescence imaging of H_2S release from Gel@GYY in the IEC-6 cells.

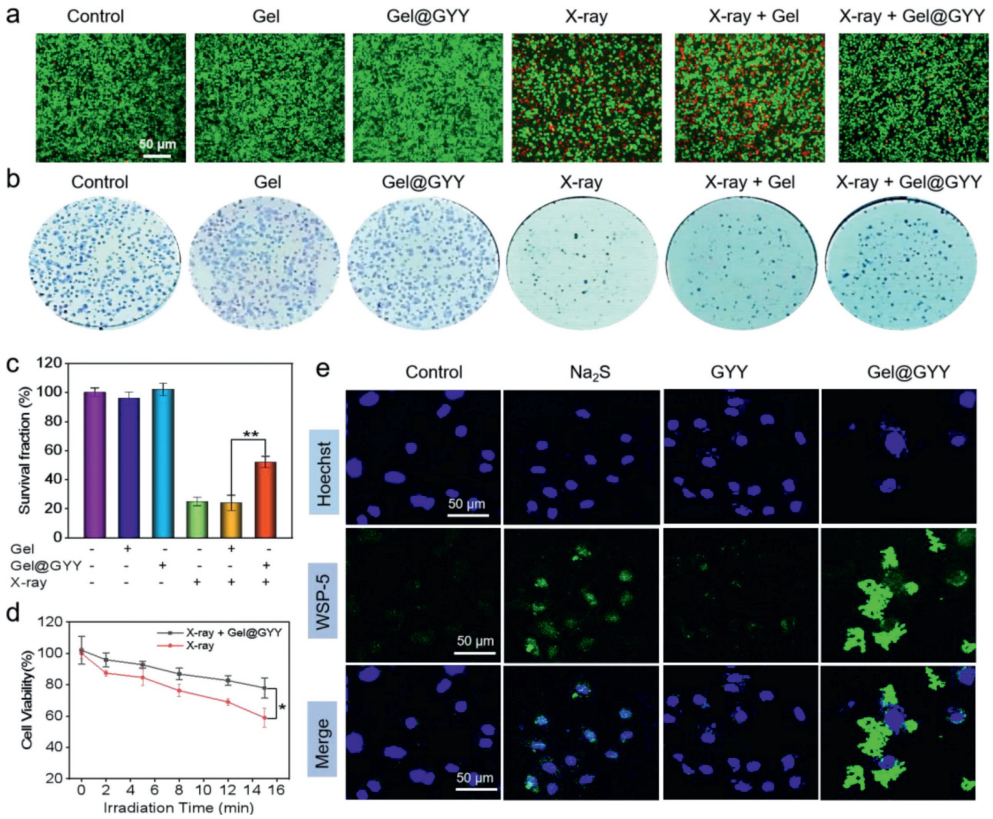

Fig. 3. Protection effect and H_2S release in IEC-6 cells. (a) Live-dead staining of IEC-6 cells with different treatments. X-ray power: 45 kV, 75 μA, 10 min. (b) Clonal survival experiments of IEC-6 cells in each group. X-ray irradiation dose: 6 Gy. (c) Responding survival fraction of IEC-6 cells in each group after 7-day colony ($^{**}P < 0.01$). (d) Cell viability of X-ray group and X-ray + Gel@GYY group at different radiation time. X-ray power: 45 kV, 75 μA, 10 min ($^{*}P < 0.05$). (e) Intracellular H_2S release detected by fluorescent imaging of differently treated IEC-6 cells using WSP-5 probe. Data represent mean ± standard error of the mean ($n = 3$).

As seen in Fig. 3e and Fig. S10 (Supporting information), control group showed weak green fluorescence due to the binding of endogenous H_2S with WSP-5. Meanwhile, both positive Na_2S group and GYY group with the same concentration were also used to incubate with the IEC-6 cells. The fluorescence intensity of GYY group was weaker than that of the Na_2S group but obviously stronger than that of the control group. This result suggested that GYY as a sustain-releasing donor released H_2S at a slower rate than the Na_2S in cells. Interestingly, the green fluorescence around the cells of the Gel@GYY group was the strongest compared to other groups, implying that Gel@GYY clustered around the cells with good adhesion ability, which was more conducive to increasing the physical distance between the released H_2S and the cells. Therefore, compared with the fast-releasing Na_2S donor, these results implied that the Gel@GYY sustainably released H_2S with an appropriate rate in cells, while Gel in the Gel@GYY promoted the GYY to gather and adhere around the cells to facilitate release and retention of H_2S, consequently improving the availability of Gel@GYY.

Based on the effective radioprotection of Gel@GYY against IEC-6 cells, we next investigated its protection mechanism. Mitochondria and DNA are the main targets of oxidative damage and their apoptosis can even be caused by oxidative damage of reactive oxygen species (ROS) [49]. Therefore, we hypothesize that the radioprotection mechanism by which Gel@GYY protects the cells from radiation damage could be due to mitigated ROS damage to mitochondria and DNA. A fluorescent probe 2,7-dichlorodi-hydro-fluorescein diacetate (DCFH-DA) was then used to detect its mitigation ability of intracellular ROS. In Figs. 4a and b, compared to control group, a significantly green fluorescence signal can be observed in X-ray irradiated IEC-6 cells, implying that a large number of ROS were generated. In marked contrast, green fluorescence signal of the X-ray + Gel@GYY group obviously decreased, but not the X-ray + Gel group. These results demonstrated that Gel@GYY has a strong ability to scavenge ROS, implying an effective intracellular H_2S release from Gel@GYY.

DNA is another major target for ROS to attack cells. Therefore, phospho-histone H2AX (γ-H2AX) closely related to DNA damage was used to determine double-stranded DNA breakage (DSBs). As shown in Figs. 4a and c, in the X-ray group, the proportion of red was significantly increased, indicating that there were significant DSBs in the IEC-6 nucleus. In contrast, DSBs of the X-ray + Gel@GYY group decreased dramatically compared to the X-ray group, which significantly suggested that Gel@GYY can effectively weaken radiation-induced DNA damage. The decrease of mitochondrial membrane potential (MMP) is a landmark event of cell apoptosis. We therefore used an MMP detection kit (JC-1) to measure whether the MMP of IEC-6 cells will change in each group. Green fluorescence produces when MMP is low but red fluorescence appears when MMP is high. In Figs. 4a and d, the fluorescence and red/green ratio indicated the change of MMP. The red/green ratio of the X-ray group was significantly lower than that of the control group, indicating a severe decrease of MMP. In contrast, red/green ratio of the X-ray + Gel@GYY group was close to that of the control group, indicating that Gel@GYY can protect mitochondria by well inhibiting the decrease of MMP. The decreased MMP can cause mitochondrial dysfunction, which releases cytochrome c for activating the apoptotic pathway. Therefore, we further studied the released cytochrome c by colocalization of cytochrome c and mitochondria (Fig. 4a). Red fluorescence and green fluorescence represent mitochondria and cytochrome c, respectively. These two fluorescence signals in the control group almost overlapped with a Pearson's correlation coefficient (PCs) of

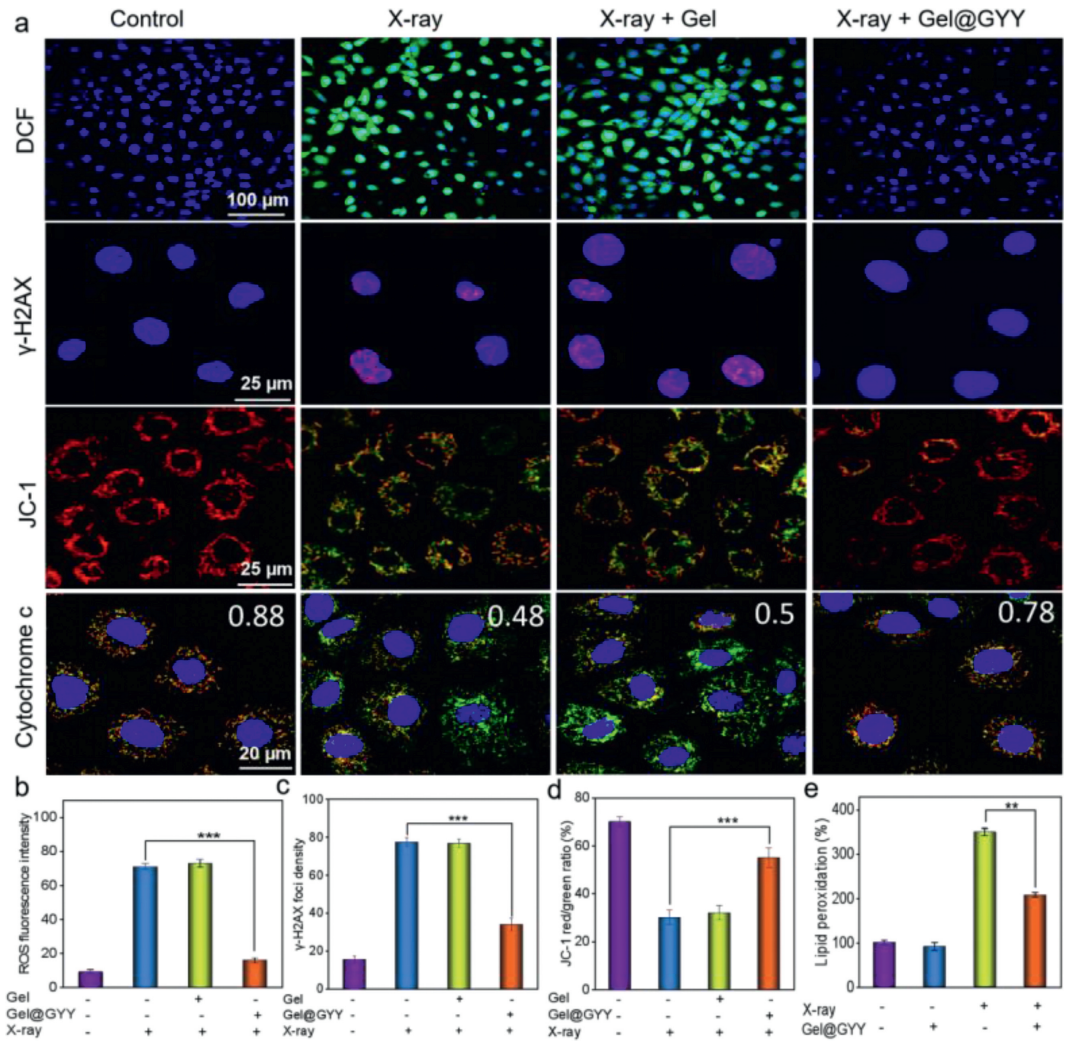

Fig. 4. Radiation protection effects and mechanism on IEC-6 cells. (a) Fluorescence images of intracellular ROS detected by DCFH-DA probe, immunofluorescence images of γ-H2AX representing DNA double-strand damage, fluorescence imaging of changes of MMP detected by JC-1, and fluorescence imaging of cytochrome c release in mitochondria after different treatments. X-ray power: 45 kV, 75 μA, 10 min. (b) Fluorescence intensity statistics of ROS of IEC-6 cells after different treatments. (c) The number of γ-H2AX foci per cell. (d) JC-1 red/green ratio in each group. (e) MDA level of lipid peroxidation after different treatments. X-ray power: 45 kV, 75 μA, 10 min ($^{**}P < 0.01$, $^{***}P < 0.001$). Data represent mean ± standard error of the mean ($n = 3$).

0.88. In contrast, these two fluorescence signals in the X-ray group sharply separated and PCs decreased to 0.48, indicating the release of cytochrome c from the mitochondria. However, the green and red fluorescence signals of the X-ray + Gel@GYY group highly overlapped and the PCs reached 0.78, which was close to the value of control group, indicating the effective inhibition of the release of cytochrome c and thereby inhibition of cell apoptosis by the Gel@GYY.

Next, we investigated the 3,4-methylenedioxyam-phetamine (MDA) level in IEC-6 cells, which is involved in LPO when cells undergo oxidative stress. In Fig. 4e, upon X-ray irradiation, the MDA level increased to 3.5 times higher than that of the control group, indicating that the radiation caused oxidative stress in the cells. On the contrary, the MDA level in the X-ray + Gel@GYY group was significantly lower than that of the X-ray group, suggesting reduced oxidative stress. As a result, Gel@GYY can effectively protect DNA and mitochondria from ROS attack, reduce radiation-induced oxidative stress and ultimately inhibit the apoptotic pathway, thus effectively mitigating the radiation-induced damage.

Retention time and biodistribution of orally administered drugs in the GI tract are important to therapeutic efficacy [50]. Therefore, we used *in vivo* fluorescence imaging to track the retention time and biodistribution of Gel@GYY in the GI tract of mouse. All animal procedures have been approved by the guideline for Care and Use of Laboratory Animals Ethical Committee at National Center for Nanoscience and Technology, Chinese Academy of Sciences. We modified Gel@GYY with fluorescent dye (Cy5) by physical cross-linking to obtain Gel@GYY@Cy5. In Fig. S11a (Supporting information), the fluorescence signal in the GI tract of oral Cy5 group significantly decreased within 4 h and almost disappeared in the stomach and intestinal tract within 6 h, which was also confirmed by fluorescence intensity statistics (Figs. S11b and c in Supporting information). However, in the oral Gel@GYY@Cy5 group in Fig. S12a (Supporting information), the fluorescence signal in the GI tract was still strong after 7 h. Based on the statistical results (Figs. S12b and c in Supporting information), the fluorescence intensity in the stomach of Gel@GYY@Cy5 group was ~60-fold higher than that of Cy5 group and the fluorescence intensity in the colon of Gel@Cy5 group was ~40-fold higher than that of the Cy5 group after 7 h. In particular, the fluorescence signals still existed in the stomach, cecum, small intestine and colon of Gel@GYY@Cy5 group after 12 h. Moreover, based on the fluorescence signal of the gastrointestinal tract in Fig. S12a, we found that the intestine especially in the colonic site was the brightest after oral Gel@GYY for 1 h, which can

be used to determine the optimal time of oral Gel@GYY for X-ray irradiation. These results showed that Gel@GYY can adhere to the GI tract for sufficient time, which facilitates its oral application in mitigating radiation damage to the GI tract.

Due to the controllable H_2S release, obvious radioprotective effect and sufficient retention time of the Gel@GYY in the GI tract, we then evaluated the biosafety of both Gel hydrogel and Gel@GYY at the cellular level. First, CCK-8 assay was used to determine the cytotoxicity of Gel hydrogel and Gel@GYY on IEC-6 cells. After incubation with IEC-6 cells for 24 and 48 h, no significant cytotoxicity was observed even the Gel@GYY and Gel hydrogel concentrations up to 4 mg/mL (Figs. S13a and b in Supporting information). Simliar results of cytotoxicity of Gel hydrogel and Gel@GYY were obtained on the human umbilical vein endothelial cells (HUVEC) (Figs. S13c and d). Then, we further studied the effect of Gel hydrogel on hemolysis of red blood cells (RBCs). The result showed that no obvious hemolytic erythrocytes were detected within the test dose (Fig. S14 in Supporting information).

To verify the effect of Gel@GYY on GI tract radiation protection, the overall *in vivo* experimental process was designed in Fig. 5a and the Kunming mice were randomly divided into Control, X-ray, Gel@GYY, and X-ray + Gel@GYY groups. Especially, a high 17 Gy X-ray irradiation dose was employed for X-ray and X-ray + Gel@GYY groups to construct radioactive gastroenteritis in mice. Moreover, disease activity index (DAI) is known to reflect the severity of inflammatory diseases. The weight and feces of different groups of mice were recorded and the statistical indices were integrated into DAI. As shown in Fig. 5c, DAI of the X-ray group was significantly increased in contrast to control group, but the DAI of X-ray + Gel@GYY group was significantly lower than that of the X-ray group, demonstrating the effective mitigation of DAI of the Gel@GYY group. On days 1, 4, and 7 after irradiation, three mice in each group were executed. Blood, stomach, colon and other major tissues were collected. Next, the tissues were weighed and the lengths of colon were measured. The mice in the X-ray group continued to lose weight while the X-ray + Gel@GYY group lost weight in the first 3 days, but recovered from day 4 and gradually returned to a similar weight to the control group and Gel@GYY group (Fig. 5b). On day 7, there was a significant difference in body weight between the X-ray group and X-ray + Gel@GYY group. The mice of X-ray treated group started to show mortality on day 6 and all of them died on day 7. In marked contrast, there were no deaths in the X-ray + Gel@GYY group. In the colon injury experiment, the length of the colon is the most visual way to determine the injury condition, and the colon was shortened as the injury worsened [45]. In Fig. 5d, the length of colon was shorter in the X-ray group than in the control group, indicating increasingly severe damage. In contrast, the colon length of X-ray + Gel@GYY treated group was longer than that of the X-ray group, suggesting that Gel@GYY can effectively reduce the irradiation damage to the colon.

The blood system is also vulnerable to radiation damage. On the 1st day, white blood cells (WBC) in the X-ray group (Fig. 5e) decreased from 6.2×10^9 to 2.6×10^9 due to the side effects of X-ray-induced inflammation to normal cells. In contrast, WBC in the X-ray + Gel@GYY group can recover to 4.9×10^9, indicating the better radioprotection effect of Gel@GYY. Other blood routine constants of the control group and X-ray group had no significant differences (Fig. S15 in Supporting information). The main blood biochemical constants including alanine aminotransferase (ALT) (Fig. 5f) and blood urea nitrogen (BUN) (Fig. 5g) in the X-ray group decreased significantly, in contrast, to the control group and significantly recovered in X-ray + Gel@GYY group. Other blood biochemical constants including creatinine (CREA) and aspartate (AST) did not show significant differences (Fig. S16 in Supporting information). These results indicated that X-ray + Gel@GYY can reduce the radiation damage to the main liver and kidney functions and immunity system. In addition, the major organ indexes were lower in the X-ray group than in the control group after irradiation, and the most significant changes in the indexes appeared in the spleen. But the indexes of each organ in the X-ray + Gel@GYY group rebounded, indicating that Gel@GYY can effectively reduce the radiation damage to the internal organs (Fig. S17 in Supporting information). The Gel@GYY can activate the protection of healthy cells by removing ROS and reducing radiation damage to organs.

To further directly verify the GI tract radioprotective effects of Gel@GYY, mouse stomach and colon were collected for pathological hematoxylin and eosin (H&E) analysis. As shown in Fig. 5h, the control group had normal colonic tissue structure with intact mucosa and well-shaped crypt and colonic villi. In contrast, during the 1st day of X-ray irradiation group, the colonic epithelium tissues began to be necrocytosis, the goblet cells appeared to die and crypt structures were damaged. On the 7th day, severe destruction of colonic epithelium tissues and structural collapse appeared. In contrast, in the X-ray + Gel@GYY group, from the 1st day after irradiation, radiation damage was significantly reduced, the morphology of the colonic epithelium tissues gradually improved, and the goblet cells and crypt structures were significantly recovered. These results indicated that radiation damage had been reduced by the Gel@GYY treatment. Similar results for the protective effect of the Gel@GYY were observed in the stomach (Fig. 5i) and small intestine (Fig. S18 in Supporting information) of mice. In Fig. 5i, the gastric tissues of the control group were intact and clear, the gastric glands were neatly arranged and the epithelial cells of the gastric mucosa were columnar in shape with no significant detachment. In the X-ray group, on the 1st day upon X-ray irradiation, apoptosis and necrosis occurred in the upper mucosal cells of the stomach, the gastric glands began to atrophy, and the number of fibrotic cells decreased. On the 7th day, the gastric wall was severely necrotic, the epidermal cells were vacuolated, the upper mucosal cells were severely necrotic, the gastric glands were extremely atrophic, and there were very few fibrotic cells. By contrast, in the X-ray + Gel@GYY group, despite the partial loss of gastric epithelial cells, the degree of atrophy of the gastric glands was greatly reduced, the cells in the upper mucosa were arranged in an orderly manner, and the myofibroblasts in the muscle layer were arranged orderly. In Fig. S18, in the control group, the small intestinal crypt and glands were well arranged and the mucosae had normal ciliated columnar epithelium and goblet cells. However, after X-ray irradiation, the structure of intestinal tissue exhibited obvious injuries and large amounts of necrosis of the small intestinal epithelial cells were observed. In contrast, the injuries were greatly relieved from the 1st to the 7th day in the Gel@GYY + X-ray group. Therefore, Gel@GYY can effectively reduce radiation-induced damage to GI tract.

Next, *in vivo* biosafety of Gel@GYY was evaluated. The body weight of mice in the Gel@GYY group did not change significantly compared to the control group (Fig. 5b). H&E staining of the main tissues showed no significant difference from normal tissues, demonstrating the superior biosafety of Gel@GYY (Fig. S19 in Supporting information). In contrast to the control group, routine blood (Fig. S20a in Supporting information) and blood biochemistry (Fig. S20b in Supporting information) analyses of the Gel@GYY group showed no obvious distinctions on day 8, demonstrating that the oral Gel@GYY was low toxic to the blood. Therefore, these results demonstrated the obvious role of the Gel@GYY in reducing radiation damage to the GI tract, making it suitable as a safe oral radioprotective agent.

Radiation exposure to the GI tract also easily leads to gastroenteritis, which in turn causes subsequent GI bleeding [51]. Therefore, we further studied the changes of GI inflammatory cytokines after X-ray irradiation. In normal cells, NF-κB is retained in the cytoplasm by binding to inhibitory kappa B (IkBs) protein in an inac-

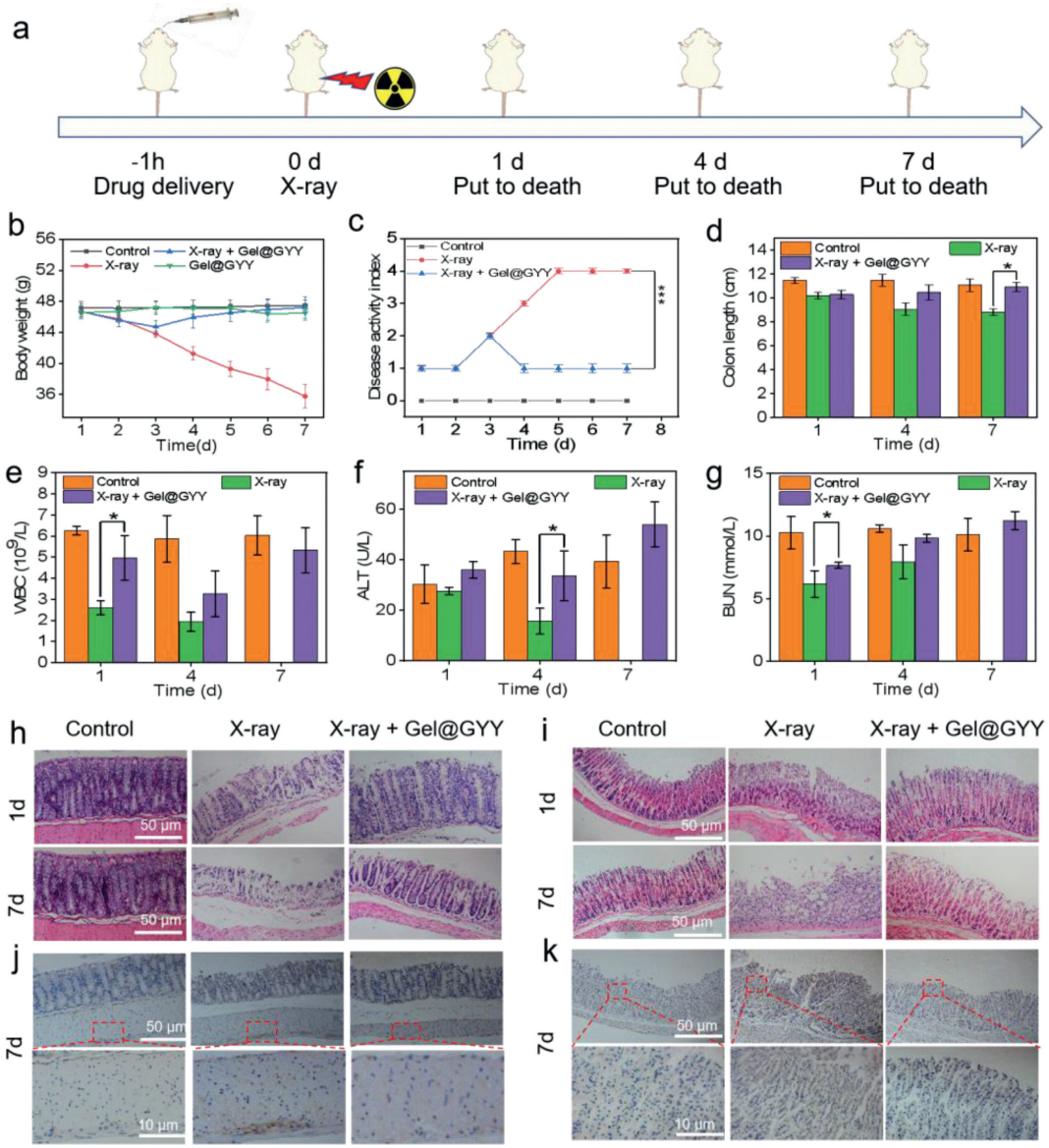

Fig. 5. Radioprotective effects in a mouse model. (a) Overall experimental procedure. (b) Changes in body weight of mice during treatment. (c) Changes of disease activity index (DAI) in each group after different treatments. (d) Length of colon tissue isolated from mice on days 1, 4 and 7 after X-ray irradiation. (e) Hematological data of WBC of mice on days 1, 4 and 7 after X-ray irradiation. Blood biochemical data of (f) ALT and (g) BUN of mice on days 1, 4 and 7 after X-ray irradiation. X-ray power: 17 Gy (*$P < 0.05$). H&E staining images of the (h) colon and (i) stomach at different time points. NF-κB immunohistochemical analysis of (j) colon and (k) stomach on the 7 day after X-ray irradiation. Data represent mean ± standard error of the mean ($n = 3$).

tive manner, thus preventing entry into the nucleus. External stimuli such as ROS could lead to phosphorylation of IkBs, resulting in the dissociation of NF-κB, causing inflammation. Previous reports displayed that H_2S has antiinflammation and antioxidant effects and the activity of NF-κB is vulnerable to the levels of H_2S [52]. Necessarily, NF-κB signal was determined to investigate the protective mechanism of Gel@GYY. As shown in Fig. 5j, NF-κB expression in the outer mucosal layer was more pronounced for X-ray group than the control group. In contrast, after being treated with Gel@GYY, NF-κB in the outer layer of the colon mucosa was significantly reduced and was near to that of the control group. In Fig. 5k, histochemical staining of the stomach after 7 days of X-ray irradiation showed that NF-κB was widely expressed in both mucosal and villi sites with significantly darker color in the X-ray group than the control group. As expected, staining in the gastric villi sites of the X-ray + Gel@GYY group was lighter than that in the X-ray group, indicating the expression of NF-κB was greatly reduced. The result suggested that the released H_2S from Gel@GYY helps to suppress NF-κB expression in the colon and stomach. Furthermore, inflammatory cytokines including tumor necrosis factor-α (TNF-α) (Fig. S21a in Supporting information) and IL-6 (Fig. S21b in Supporting information) in the colon were gradually elevated on days 1, 4, and 7 after radiation. However, the inflammatory factors levels of the X-ray + Gel@GYY group were significantly lower than those in the X-ray group. Also, the tendency of inflammatory factors in the stomach on day 7 was similar to the colon tissues (Figs. S21c and d in Supporting information). All these results demonstrated that the controllable pH-responsive and sustainable releasing H_2S from Gel@GYY in the GI tract can significantly and effectively suppress the expression of NF-κB in stomach and colon, which in turn reduced the level of inflammation induced by X-ray radiation.

Oxidative stress is mainly induced by increased ROS, which can result in extensive injury to cells by attacking proteins, DNA and lipids. In normal physiological system, ROS can be neutralized

by antioxidant defense systems including various antioxidant enzymes. Radiation exposure to the GI tract can cause the reduction of the activity of various antioxidant enzymes. SOD is an important antioxidant enzyme that can catalyze $O_2^{-\bullet}$ disproportionation to generate H_2O_2 and O_2 [53]. As shown in Figs. S21e and f (Supporting information), at 1, 4 and 7 days after X-ray irradiation, the SOD levels decreased in the colon and stomach in the X-ray group, and the decrease was increasingly pronounced compared to the control group. As expected, the SOD levels started to gradually recover after Gel@GYY treatment, suggesting that Gel@GYY with enhanced antioxidant capacity to the colon and stomach can reduce the damage of SOD. Glutathione peroxidase (GSH-Px) is another important antioxidant enzyme in many living cells. The physiological function of GSH-Px is to catalyze GSH to participate in peroxide reactions to eliminate free radicals [54]. In Figs. S21g and h (Supporting information), GSH-Px activity of the colon and stomach in the X-ray group gradually decreased within 7 days and the activity was weaker than that of the control group. However, in the X-ray + Gel@GYY group, GSH-Px activity recovered to some extent, indicating that the Gel@GYY is beneficial to mitigating the damage of radiation, reducing oxidation levels and protecting gastric and colonic tissues. It has been reported that the Gel hydrogel has the effect of promoting cell adhesion and production, good affinity to biological tissues and good hemostatic effect [55]. We therefore investigated the hemostatic effect of the oral Gel hydrogel. As shown in Fig. S22a (Supporting information), the bleeding volume on the filter paper in the hemostasis group of Gel hydrogel was smaller than that of the control group within 120 s. Statistically, the amount of blood loss in the Gel hydrogel group was nearly half of that in control group in Fig. S22b (Supporting information), indicating that the Gel hydrogel helps to protect against radiation-induced GI bleeding. In this case, the protective effects of Gel@GYY on GI tract can be attributed to its superior abilities to enhance the retention time of H_2S in the GI tract, scavenging free radicals, suppressing radiation-induced inflammatory factors, recovering the SOD and GSH-Px activity, and preventing possible GI bleeding caused by late radiation of GI tract.

In summary, we have developed an oral radioprotectant comprising porous Gel hydrogel loaded H_2S donor GYY (Gel@GYY) that can effectively reduce the damage to GI tract caused by X-ray radiation. After oral administration, the biocompatible Gel@GYY had good adhesion in the GI tract followed by the controllable release of H_2S through pH-response in the gastric environment and sustained release of H_2S in the whole intestinal tract, especially in the colon of mice. Moreover, Gel@GYY can effectively scavenge toxic free radicals through the controllably released H_2S, consequently reducing free radicals-induced damage to DNA and mitochondria. Animal experiments also showed that the Gel@GYY effectively inhibited the activation of NF-κB, thus reducing the level of radiation-induced inflammatory factors. In particular, the good adhesion ability of Gel@GYY increased the physical distance between the released H_2S and the GI tract, which in turn improved the availability of H_2S. In addition, Gel@GYY helped the recovery of the SOD and GSH-Px levels to reduce oxidative stress, protecting the whole GI tract. The Gel hydrogel in Gel@GYY can reduce radiation-induced GI tract bleeding and be readily degradable with good biosafety *in vivo*. Our study provides an intelligent H_2S-releasing delivery system Gel@GYY as a potential oral GI tract radioprotective agent in the clinical conversion of H_2S.

Declaration of competing interest

The authors declare that they have no known competing financial interests or personal relationships that could have appeared to influence the work reported in this paper.

Acknowledgments

This work was supported by the National Natural Science Foundation of China (Nos. 22175182, 21471103), Sheng Yuan Cooperation (No. 2021SYHZ0048), Beijing Natural Science Foundation (No. 2202064), and the directional institutionalized scientific research platform relies on Beijing Synchrotron Radiation Facility of Chinese Academy of Sciences.

Supplementary materials

Supplementary material associated with this article can be found, in the online version, at doi:10.1016/j.cclet.2023.108545.

References

[1] D. Zhang, D. Zhong, J. Ouyang, et al., Nat. Commun. 13 (2022) 1413.
[2] W. Fu, X. Zhang, L. Mei, et al., ACS Nano 14 (2020) 10001–10017.
[3] S.L. Warren, G.H. Whipple, J. Exp. Med. 35 (1922) 187–202.
[4] M. Teo, D. Sebag-Montefiore, C.F. Donnellan, Clin. Oncol. 27 (2015) 656–667.
[5] J.M. Novak, J.T. Collins, M. Donowitz, et al., J. Clin. Gastroenterol. 1 (1979) 9–40.
[6] M.I. Koukourakis, Anticancer Drugs 13 (2002) 181–209.
[7] J. Xie, Y. Yong, X. Dong, et al., ACS Appl. Mater. Inter. 9 (2017) 14281–14291.
[8] E. Seifter, J. Mendecki, S. Holtzman, et al., Pharmacol. Ther. 39 (1988) 357–365.
[9] J. Du, Z. Gu, L. Yan, et al., Adv. Mater. 29 (2017) 1701268.
[10] D. Zetner, L. Andersen, J. Rosenberg, Drug Res. 66 (2016) 281–296.
[11] K.N. Mishra, B.A. Moftah, G.A. Alsbeih, Biomed. Pharmacother. 106 (2018) 610–617.
[12] P. Haddad, B. Kalaghchi, F. Amouzegar-Hashemi, Radiother. Oncol. 77 (2005) 324–326.
[13] R.Salvador E.Obrador, J.I. Villaescusa, et al., Biomedicines 8 (2020) 461.
[14] C. Wang, J. Xie, X. Dong, et al., Small 16 (2020) 1906915.
[15] S. Han, S. Lee, M. Cho, et al., Adv. Mater. 32 (2020) 2001566.
[16] J. Colon, N. Hsieh, A. Ferguson, et al., Nanomedicine 6 (2010) 698–705.
[17] H. Liu, J. Wang, Y. Jing, et al., Part. Part. Syst. Charact. 34 (2017) 1700035.
[18] X. Ren, M. Huo, M. Wang, et al., ACS Nano 13 (2019) 6438–6454.
[19] X. Zhang, J. Zhang, J. Wang, et al., ACS Nano 10 (2016) 4511–4519.
[20] J. Wang, X. Mu, Y. Li, et al., Small 14 (2018) 1703736.
[21] S. Hua, Front. Pharmacol. 11 (2020) 524.
[22] C. Szabo, Nat. Rev. Drug Discov. 6 (2007) 917–935.
[23] V.S. Lin, W. Chen, X. Ming, et al., Chem. Soc. Rev. 44 (2015) 4596–4618.
[24] F. Rong, T. Wang, Q. Zhou, et al., Bioact. Mater. 19 (2023) 198–216.
[25] F. Ghanbari, M. Khaksari, G. Vaezi, et al., J. Mol. Neurosci. 67 (2019) 133–141.
[26] W. Liang, J. Chen, L. Li, et al., ACS Appl. Mater. Inter. 11 (2019) 14619–14629.
[27] V. Citi, E. Piragine, L. Tastai, et al., Curr. Med. Chem. 25 (2018) 4380–4401.
[28] H. Wei, X. Li, X. Tang, J. Clin. Neurosci. 21 (2014) 1665–1669.
[29] Y.Lu X.Wu, B. Liu, et al., Chin. Chem. Lett. 32 (2021) 2380–2384.
[30] L. An, X. Wang, X. Rui, et al., Angew. Chem. Int. Ed. 57 (2018) 15782–15786.
[31] J. Li, L. Xie, W. Sang, et al., Angew. Chem. Int. Ed. 61 (2022) e202200830.
[32] A. Sivarajah, M. Collino, M. Yasin, et al., Shock 31 (2009) 267–274.
[33] Y. Huang, H. Li, X. He, et al., Chin. Chem. Lett. 31 (2020) 787–791.
[34] J.L. Greaney, J.L. Kutz, S.W. Shank, et al., Hypertension 69 (2017) 902–909.
[35] D.J. Polhemus, Z. Li, C.B. Pattillo, et al., Cardiovasc. Ther. 33 (2015) 216–226.
[36] J.L. Wallace, P. Nagy, T.D. Feener, et al., Br. J. Pharmacol. 177 (2020) 769–777.
[37] L. Li, M. Whiteman, Y. Guan, et al., Circulation 117 (2008) 2351–2360.
[38] Y.W. Won, Y.H. Kim, J. Control. Release 127 (2008) 154–161.
[39] J.R. Adams, S. Senapati, S.L. Haughney, et al., J. Biomed. Mater. Res. A 107 (2019) 1754–1762.
[40] C. Tondera, S. Hauser, A. Krüger-Genge, et al., Theranostics 6 (2016) 2114–2128.
[41] L. Li, Y. Du, Z. Yin, et al., Colloids Surf. B 187 (2020) 110641.
[42] B. Naidu, A.T. Paulson, J. Appl. Polym. Sci. 121 (2011) 3495–3500.
[43] S.K. Bhattacharyya, M. Dule, R. Paul, et al., ACS Biomater. Sci. Eng. 6 (2020) 5662–5674.
[44] S. Zhao, Y. Li, Q. Liu, et al., Adv. Funct. Mater. 30 (2020) 2004692.
[45] H. Staroszczyk, K. Sztuka, J. Wolska, et al., Acta A Mol. Biomol. Spectrosc. 117 (2014) 707–712.
[46] E.M. Krop, M.M. Hetherington, M. Holmes, et al., Food Hydrocoll 88 (2019) 101–113.
[47] B. Yang, Y. Chen, J. Shi, Chem. Rev. 119 (2019) 4881–4985.
[48] P.M. Kidd, Altern. Med. Rev. 2 (1997) 155–176.
[49] H. Rottenberg, J.B. Hoek, Aging Cell 16 (2017) 943–955.
[50] H. Gunaydin, M. Altman, J.M. Ellis, et al., ACS Med. Chem. Lett. 9 (2018) 528–533.
[51] N. Hekim, Z. Cetin, Z. Nikitaki, et al., Cancer Lett. 368 (2015) 156–163.
[52] X. Zhao, L. Ning, X. Zhou, et al., Anal. Chem. 93 (2021) 4894–4901.
[53] Q. Zhang, H. Tao, Y. Lin, et al., Biomaterials 105 (2016) 206–221.
[54] M. Zu, D. Xie, B. Canup, et al., Biomaterials 279 (2021) 121178.
[55] R. Hajosch, M. Suckfuell, S. Oesser, et al., J. Biomed. Mater. Res. 94B (2010) 372–379.